



Statistical Modeling of the 3D Geometry and Topology of Botanical Trees

Guan Wang^{†1,2}, Hamid Laga^{‡2} , Jinyuan Jia^{§1}, Ning Xie^{¶3}  and Hedi Tabia^{||4}

¹Tongji University, China. ²Murdoch University, Australia. ³University of Electronic Science and Technology of China. ⁴ETIS UMR 8051, Paris Seine University, University of Cergy-Pontoise, ENSEA, CNRS, France

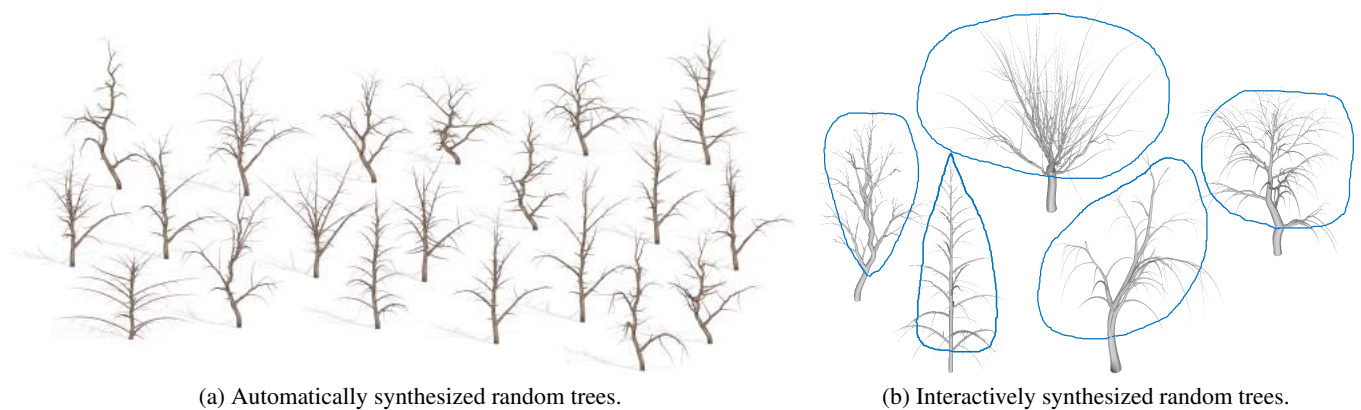


Figure 1: We take a population of 3D botanical tree models, learn their geometric and topological variability, and then synthesize new botanical trees either (a) randomly by sampling from probability distributions fitted to the population, or (b) interactively, using a 2D sketching interface, by learning regression models.

Abstract

We propose a framework for statistical modeling of the 3D geometry and topology of botanical trees. We treat botanical trees as points in a tree-shape space equipped with a proper metric that captures the geometric and the topological differences between trees. Geodesics in the tree-shape space correspond to the optimal sequence of deformations, i.e. bending, stretching, and topological changes, which align one tree onto another. In this way, the 3D tree modeling and synthesis problem becomes a problem of exploring the tree-shape space either in a controlled fashion, using statistical regression, or randomly by sampling from probability distributions fitted to populations in the tree-shape space. We show how to use this framework for (1) computing statistical summaries, e.g. the mean and modes of variations, of a population of botanical trees, (2) synthesizing random instances of botanical trees from probability distributions fitted to a population of botanical trees, and (3) modeling, interactively, 3D botanical trees using a simple sketching interface. The approach is fast and only requires as input 3D botanical tree models with a known upright orientation.

Categories and Subject Descriptors (according to ACM CCS): I.3.3 [Computer Graphics]: Picture/Image Generation—Line and curve generation

Keywords: 3D tree synthesis, regression, statistical summaries, tree-shape space, geodesics.

[†] guan.wang@tongji.edu.cn

[‡] H.Laga@murdoch.edu.au

[§] jyjia@tongji.edu.cn

[¶] seanxiening@gmail.com

^{||} hedi.tabia@ensea.fr

1. Introduction

Vegetations, which are prevalent in natural and urban environments, add a high level of realism to digital contents and virtual worlds. Creating realistic vegetations that are as rich as those seen in the real world has been actively investigated for many years. Plants, however, have complex geometry, topological structure, and appearance. As such, although there are several tools which provide interfaces for the interactive modeling of vegetations, the task is still complex and time consuming especially for novice users who do not have 3D modeling skills or biological knowledge.

In this article, we propose a data-driven approach for synthesizing new 3D botanical trees from existing ones. The approach starts with a collection of botanical trees, models the geometric and topological variability in the collection by representing the trees as points in a tree-shape space, and then synthesizes new trees either by randomly sampling from probability distributions fitted to the population in the tree-shape space, or by learning regression models which map a few (meaningful) parameters to points in the tree-shape space. This approach is very popular in the case of manifold surfaces, e.g. human faces [BV99], human body shapes [ACP03, LXJS17], and anatomical organs where variability can be captured by modeling geometric deformations such as bending and stretching [LKSM14, LXJS17]. Botanical trees are more complex since they deform in geometry, by bending and stretching their branches, and in topology since two trees, even if they belong to the same species, can have a different number of branches.

The main ingredients needed for implementing such framework are (1) a mechanism for computing one-to-one correspondences between botanical trees, (2) a concept of tree-shape space where botanical trees are represented as points, (3) a metric in the tree-shape space for quantifying geometric and topological dissimilarities, (4) a mechanism for computing optimal deformations, i.e. geodesics under the metric, between pairs of trees, (5) a mechanism for statistical modeling in the tree-shape space, and (6) a mechanism for performing regressions in the tree-shape space.

The first four problems have been investigated in [WLX*18] and [FOP*13, FLdB*13], which proposed a tree-shape space and a metric on this space for computing geodesics between tree-like shapes. Their formulation, however, uses the Quotient Euclidean Distance (QED), which, although having nice mathematical properties (such as the uniqueness of the geodesics under this metric), is not suitable for modeling the elasticity (bending and stretching) of the branches, see Figure 3. In this article, we first extend the framework of [FOP*13, FLdB*13, WLX*18] by introducing a new elastic metric, which leads to better geodesics between botanical trees that bend, stretch and deform in topology. We then use this framework to develop a mechanism for the statistical modeling of botanical trees and for performing regressions in the tree-shape space. We show that the framework can be used to synthesize random trees and to model 3D trees by using a simple 2D sketching interface.

1.1. Related work

The framework proposed in this article can be seen as the generalization of the techniques proposed for the statistical analysis of manifold 3D shapes, which bend and stretch, to botanical trees,

which vary not only in geometry but also in topology. Thus, we focus our survey on the techniques which have been proposed for modeling 3D botanical trees, and on statistical 3D shape analysis. For a more comprehensive review of the state-of-the-art of 3D tree modeling, we refer the reader to [PBI*16].

3D tree modeling. Broadly, 3D tree modeling techniques fall into two main categories; the techniques in the first category aim to reconstruct real-world 3D tree models from images [QTZ*06, TFX*08, LDS*11] or scanned point clouds [PGW*04, BL08, PSTV09, LYO*10]. Techniques in the second category, which are more relevant to the approach we propose in this article, focus on modeling and animating, automatically or interactively using 2D or 3D sketching interfaces, botanical trees with a certain level of realism [CNX*08, WBCG09, LRBP12].

One of the most popular approaches is procedural modeling, which simulates the 3D geometry and topology of complex plants by defining and then executing, repetitively, a set of rules. A popular example is the L-systems, which were originally introduced in [Lin68] as a mechanism for representing growth processes in nature. Later, L-Systems have been used by Prusinkiewicz et al. [PHHM96] to model the geometry and topological structure of trees. Lintermann and Deussen [LD99] followed this work and proposed an interface for creating 3D tree models by defining and setting a set of parameters, which can be biologically motivated. Although very powerful, modeling using L-systems requires domain expertise and knowledge of the various parameters that drive procedural models in general. More importantly, the parameterization of complex 3D tree models is a difficult issue due to the complexity of the involved biological processes and the complexity of the interactions between these processes [CLM*11].

Instead of manually tuning the parameters of a procedural model, inverse procedural modeling techniques [IMIM08, ŠBM*10, TYK*12, MVG13, SPK*14] estimate these parameters from experimental data, e.g. images and range scans, of real trees. Stava et al. [ŠBM*10], for example, proposed a compact parametric procedural model, which describes a wide variety of trees, and a Monte Carlo Markov Chain (MCMC)-based optimization method for estimating these parameters for a given tree. The estimated parameters can then be used to generate a wide variety of tree models. Several other procedural modeling methods take into account the environmental parameters and the interaction of plants with their environment. Examples include the method of [RLM07], which simulates climbing plants and their response to light density, and the approach of [PSK*12], which employs environmental sensitivity to static input trees and allows the user to automatically change the tree topology under varying environmental conditions.

Sketch-based techniques have been also used to create and animate, interactively, 3D models of trees [PBPS99, PMK-L01, CNX*08, OOI07, LRBP12]. These techniques often use biologically-motivated rules to infer the 3D geometry and topology of trees from 2D or 3D sketches drawn by the user. Thus, similar to rule-based and procedural modeling techniques, rules need to be explicitly specified. The framework proposed in this article also enables sketch-based tree synthesis. However, instead of explicitly specifying the rules, we formulate the problem using regressions. Thus, such rules are implicitly discovered from training data.

Finally, several techniques have been proposed to model the effect on the shape and growth of trees of external stresses such as wind [PNH*14] and obstacles [HBDP17]. Others considered the problem of animating trees and plants [QYH*17, HBDP17]. Our approach focuses on the process of creating 3D tree models. The models generated with our approach can then be fed into other tools for animation and interaction with their environments.

Statistical shape analysis and exploration. In general, learning the parameters of a procedural model is computationally expensive. In this article, we take a different approach. We take examples of trees that belong to the same family and learn their geometric and topological variability by fitting to the collection a probability model. The synthesis of new instances is then reduced to the problem of sampling from the probability distribution. This idea has been investigated in the case of manifold 3D shapes such as human faces [BV99], human body shapes [ACP03, LXJS17, JKLS17], as well as general manifold shapes [KSKL13, LXJS17, ZHRS15]. These methods, however, are limited to 3D models that bend and stretch. They do not capture structural variabilities such as those present in botanical trees.

The approach we propose in this article builds on the recent theoretical developments in graph and tree statistics, pioneered by Billera et al. [BHV01], which proposed the concept of continuous tree-space and its associated distance metrics and computational tools for computing geodesics and summary statistics. This concept has been used by various authors for the statistical analysis of tree-structured data, e.g. [OP11] and [AAV*14]. However, these works focused only on the topological structure ignoring the geometry and shape of the edges. Feragen et al. [FLdB*13, FOP*13] extended this concept and proposed a tree-shape space and a set of metrics for computing statistics of airway trees. Due to their computational complexity, these methods are restricted to relatively small trees that exhibit only minor structural differences.

Wang et al. [WLX*18] extended the work of Feragen et al. [FLdB*13] by providing a practical implementation, which enabled the computation of geodesics between very complex botanical trees. Both [FLdB*13] and [WLX*18] used the Quotient Euclidean Distance as a metric. We show in this article that this metric is not suitable for capturing large deformations and propose a new full elastic metric. Also, Wang et al. [WLX*18] focused only on the computation of geodesics and mean trees. In this article, we develop a full statistical analysis framework.

Finally, there have been a few works that attempted computing smooth deformations between 3D shapes which deform in geometry and topology. Examples include the work of [AXZ*15] for man-made 3D shapes, and its extension to botanical trees [WXJD17]. These works, however, do not come with a concept of a shape space and a metric. Thus, while they can compute nice blending between 3D shapes, they cannot be used for full statistical analysis or regression as proposed in this article.

1.2. Overview and contributions

Similar to Wang et al. [WLX*18], we treat a 3D botanical tree as a point in a high-dimensional tree-shape space, equipped with

a metric that quantifies geometric and topological differences between tree-like shapes (Section 2). Unlike Wang et al. [WLX*18], we propose a new elastic metric which is more suitable for capturing, in addition to topological deformations, large elastic deformations, i.e. the bending and stretching of tree branches. Having a proper tree-shape space, a metric, and a mechanism for computing geodesics enables us to perform full statistical modeling of the geometric and structural variabilities in a collection of 3D botanical trees (Sections 3.1 and 3.2). It also facilitates 3D modeling tasks. We show that statistical modeling in the tree-shape space can be used for synthesizing, in an automated manner, new instances of botanical trees with rich geometric and structural details (Section 3.3). We also formulate the problem of inferring full 3D trees from 2D sketches as a regression problem in the tree-shape space and develop a sketching interface, which facilitates the 3D modeling process (Section 4). The main contributions of this article can be summarized as follows;

- We introduce a new elastic metric, which captures the elastic deformations of the tree branches as well as the topological deformations of the trees. Unlike the QED metric of Feragen et al. [FOP*13, FLdB*13] and used by Wang et al. [WLX*18], the new metric is suitable for computing geodesics between botanical trees that undergo large geometric and topological deformations.
- We introduce a new tree-shape space called the *Extended Square Root Velocity Function (ESRVF)* tree-shape space, and show that, in this space, the complex elastic metric reduces to the simple Quotient Euclidean Distance (QED). As a result, geodesics can be first computed in the ESRVF space and then mapped back to the original space of trees. We show that this new formulation leads to better results compared to Wang et al. [WLX*18].
- We build on this formulation a framework for the statistical analysis of populations of botanical trees. The framework enables computing summary statistics. In other words, it enables abstracting collections of botanical trees by producing means and principal modes of variation, which reveal geometric and topological variation trends inside the collection. It also enables characterizing populations of trees with probability distributions, which in turn can be used to generate random instances of 3D botanical trees. These cannot be achieved using previous techniques such as inverse procedural modeling [SBM*10, SPK*14] or structural blending [WXJD17].
- We develop a mechanism for regressions in the tree-shape space. Using this mechanism, we develop a simple 2D sketching interface to model, interactively, 3D botanical trees.

2. The ESRVF tree-shape space

In this section, we will review the construction of the tree-shape space, propose a new metric, and then overview the mechanism for computing geodesics. The first and last points have been already discussed in [WLX*18]. The new metric, which we propose in this article in order to handle botanical trees which undergo large deformations, is a major extension, compared to [WLX*18].

2.1. Representation

The input to our framework is a set of 3D polygonal models of botanical trees. We first skeletonize each tree using the skeletonization approach of Zhang et al. [ZXLJ15], and then convert it into a tree-graph $G = (V, E, A)$. Here, V is the set of nodes, which are either branch extremities or bifurcation points. Each non-oriented edge e in E , which connects a pair of nodes, is augmented with shape attributes in A . In this article, we represent the shape of an edge e using its skeletal curve augmented with the local thickness at each skeletal point. Thus, the shape attributes of an edge e is a function of the form $x_e : [0, 1] \rightarrow \mathbb{R}^3 \times \mathbb{R}^+$. Let \mathcal{F}_e denote the space of such curves. \mathcal{F}_e has an infinite dimension since its elements are continuous functions.

Following the approach of [FLL*11], we first convert the tree-graph G of each botanical tree into a binary tree and then into a maximal binary tree, i.e. a tree where each node has three incident edges, except the root, which has only two, and the leaf nodes, which have only one. We do so by adding virtual nodes and edges. (Here, we define a virtual edge as the edge whose shape attributes are all set to zero). Amongst these maximal binary trees, we select the largest one. All the other trees are then parameterized with this maximal binary tree by adding virtual nodes and edges. This will ensure a common parameterization of all the botanical trees of the collection. Note that, as discussed in [WLX*18], this parameterization is not unique. Hereinafter, and for simplicity, we denote by G the tree graph which represents a given 3D botanical tree.

This representation has two important properties; First, every botanical tree \mathbf{x} is parameterized with the maximal graph $G_{\mathbf{x}} = (V, E, A_{\mathbf{x}})$. The pair (V, E) are common to all trees. What differs between a botanical tree \mathbf{x} and another botanical tree \mathbf{y} is their attributes $A_{\mathbf{x}}$ and $A_{\mathbf{y}}$, respectively. Second, all botanical trees become points in the tree-shape space $X = \mathcal{F}_{e_1} \times \dots \times \mathcal{F}_{e_m}$, where m is the total number of edges in the maximal binary tree. As discussed in [FLL*11, FHNL11, FLdB*13], this tree-shape space can be seen as the union of orthants. Each orthant of dimension k and spanned by a set of edges e_{i_1}, \dots, e_{i_k} , is defined as $X_k = \mathcal{F}_{e_{i_1}} \times \dots \times \mathcal{F}_{e_{i_k}}$. A projection along one dimension, say \mathcal{F}_e , is equivalent to setting the shape attributes of e to zero. This corresponds to an edge collapse. On the other hand, adding a new dimension is equivalent to expanding or inserting an edge. Thus, points within the same orthant correspond to tree-shapes which have the same structure. Paths within the same orthant correspond to the bending and stretching of the edges which span that orthant while preserving the topology of the tree. A transition from one orthant to another of lower dimension is equivalent to collapsing edges while a transition to an orthant of higher dimension corresponds to the insertion of new edges. This is illustrated in Figure 2-(a).

2.2. Metrics and geodesics

Let \mathbf{x} and \mathbf{y} be two points in X . Let $\alpha : [0, 1] \rightarrow X$ be a parameterized path in X such that $\alpha(0) = \mathbf{x}$, $\alpha(1) = \mathbf{y}$, and $\forall t \in [0, 1], \alpha(t) \in X$. First, let us assume that \mathbf{x} and \mathbf{y} are on the same orthant and thus have the same topology. If the edges of the trees represented by \mathbf{x} and \mathbf{y} are (e_1^x, \dots, e_m^x) and (e_1^y, \dots, e_m^y) , respectively, then the length

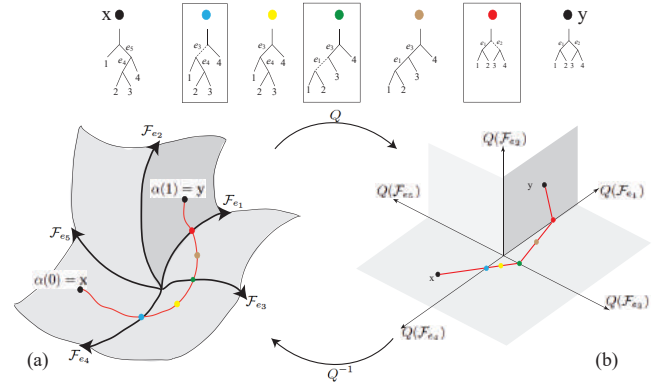


Figure 2: (a) The tree-shape space X , which is equipped with the non-linear elastic metric, and (b) its mapping into the ESRVF tree-shape space Ω , which is equipped with the QED metric. Paths within the same orthant correspond to geometric deformations (e.g. bending and stretching), while transitions from one orthant to another correspond to topological deformations, e.g. addition or suppression of edges. In this example, the trees highlighted in the top of the figure correspond to topological transitions.

of α , hereinafter denoted by $L[\alpha]$, is given by:

$$L[\alpha_{\mathbf{x} \rightarrow \mathbf{y}}] = \left(\sum_{i=1}^m L[\beta_{e_i^x \rightarrow e_{\phi(i)}^y}]^a \right)^{\frac{1}{a}}, \quad (1)$$

where $a \in \mathbb{R}_{>0}$ and $\beta_{e_i^x \rightarrow e_{\phi(i)}^y}$ is the path which deforms the shape of the edge e_i^x in \mathbf{x} onto its corresponding edge $e_{\phi(i)}^y$ in \mathbf{y} . (In other words, ϕ provides correspondences between the edges of \mathbf{x} and the edges of \mathbf{y} .) The length $L[\beta_{e_i^x \rightarrow e_{\phi(i)}^y}]$ of the path $\beta_{e_i^x \rightarrow e_{\phi(i)}^y}$ is given by

$$L[\beta] = \int_0^1 \langle \dot{\beta}(t), \dot{\beta}(t) \rangle^{\frac{1}{2}} dt, \quad (2)$$

where $\langle \cdot, \cdot \rangle$ is a certain metric and $\dot{\beta} = \frac{\partial \beta}{\partial t}$ is the velocity vector. (Note that here we dropped the indices of the path β for clarity.)

Since both trees are within the same orthant, the path α corresponds to deformations in the shape of the edges while keeping the topological structure constant. Now if \mathbf{x} and \mathbf{y} have different topologies, then a path which connects them will be composed of N segments, each one belongs to one orthant, see Figure 2-(a). The length of the path is the sum of the lengths of these path segments:

$$L[\alpha_{\mathbf{x} \rightarrow \mathbf{y}}] = \sum_{t=1}^{N-1} L[\alpha_{\mathbf{x}_t \rightarrow \mathbf{x}_{t+1}}], \quad (3)$$

where $\mathbf{x}_1 = \mathbf{x}$, $\mathbf{x}_N = \mathbf{y}$, and \mathbf{x}_t and \mathbf{x}_{t+1} , for $t > 1$ and $t < N$, sit on the boundaries of the same orthant. Since \mathbf{x}_t and \mathbf{x}_{t+1} are on the same orthant then the length of the path segment $\alpha_{\mathbf{x}_t \rightarrow \mathbf{x}_{t+1}}$ is given by Equation (1).

In our analysis, we are interested in the shortest path, i.e. the path $\alpha^* = \arg \min_{\alpha} L[\alpha_{\mathbf{x} \rightarrow \mathbf{y}}]$, hereinafter called the *geodesic*, under the metric $\langle \cdot, \cdot \rangle$ of Equation (2). The quality of the geodesic depends on the choice of the metric. Feragen et al. [FLdB*13] introduced

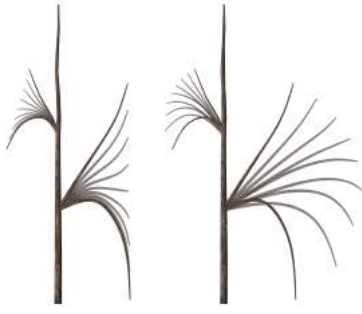


Figure 3: Comparison between a geodesic computed with the approach of [WLY*18] (left), and the approach proposed in this article (right). In both cases, the intermediate trees along the geodesic are rendered in a transparent color.

the Quotient Euclidean Distance (QED), which is defined by setting $a = 2$ and thus $\langle \dot{\beta}(t), \dot{\beta}(t) \rangle = \langle \dot{\beta}(t), \dot{\beta}(t) \rangle$, where $\langle \cdot, \cdot \rangle$ is the standard inner product between two vectors in the Euclidean space. In other words, Feragen et al. assume that the shape x of an edge of the graph G is a point in the Euclidean space, which is equipped with the \mathbb{L}^2 metric. The QED ensures that geodesics exist and are locally unique [FLdB*13]. The \mathbb{L}^2 metric, however, does not capture the natural deformations of branches. This is illustrated in the left panel of Figure 3 where one can see that when the branches significantly bend, the intermediate shapes shrink unnaturally.

The elastic metric. In this article, we propose to use an elastic metric, which captures the bending and stretching of the graph edges. Let $x : [0, 1] \rightarrow \mathbb{R}^3 \times \mathbb{R}^+$ be a representation of the shape of an edge e in G . We can write $x(s) = (f(s), r(s))$ where $f : [0, 1] \rightarrow \mathbb{R}^3$ and $r : [0, 1] \rightarrow \mathbb{R}^+$. Geometrically, f represents the skeleton of the branch while r is its thickness at each point on the skeletal curve. Consider a path $\beta_{x \rightarrow y}$, which deforms the shape x of an edge onto another shape y . (Note also that $\beta(0) = x, \beta(1) = y$). Its length $L[\beta]$ is given by Equation (2). However, instead of using the \mathbb{L}^2 metric as in [FLdB*13] and [WLY*18], we propose a new metric which quantifies the bending and stretching of the graph edges.

Physically, bending can be quantified by measuring changes in the orientation of the tangent vectors to f . Stretching can be decomposed into two components; the first one is related to the elongation of the skeletal curve, which can be quantified by looking at how the magnitude of the tangent vector to f at every point s changes. The second component is related to changes in the thickness of the branch and can be measured by looking at how r varies at each point. Let us write

$$f'(s) = \frac{\partial f(s)}{\partial s} = \theta(s)e^{\phi(s)}, \quad (4)$$

where $\theta(s)$ is the unit tangent vector to f at s , and $e^{\phi(s)}$ is the magnitude of the tangent vector to f at s . (We also refer to $e^{\phi(s)}$ as the speed.) In other words:

$$e^{\phi(s)} = \|f'(s)\| = \left\| \frac{\partial f(s)}{\partial s} \right\|, \text{ and } \theta(s) = \frac{f'(s)}{\|f'(s)\|}. \quad (5)$$

One can then define an elastic metric as the weighted sum of the

changes of ϕ , θ , and r along the path β . In other words:

$$\langle \dot{\beta}, \dot{\beta} \rangle \equiv a \int \langle \theta'(s), \theta'(s) \rangle e^{\phi(s)} ds + b \int \phi'(s)^2 e^{\phi(s)} ds + c \int r'(s)^2 e^{\phi(s)} ds. \quad (6)$$

Here, g' denotes the derivative of the function g with respect to the parameter s . The first term of Equation (6) quantifies bending by measuring changes in the orientation of the tangent vector. The second and third terms quantify stretching. The first two terms are equivalent to the elastic metric between curves in \mathbb{R}^3 , which has been introduced by Srivastava et al. [SKJJ11]. While the full elastic metric of Equation (6) is the most appropriate for analyzing the shape and topological structure of trees, it is computationally very expensive. To reduce the computation time, Srivastava et al. [SKJJ11] defined the Square Root Velocity Function (SRVF) of a curve f as:

$$q(s) = \frac{f'(s)}{\|f'(s)\|^{\frac{1}{2}}}. \quad (7)$$

More importantly, they showed that the \mathbb{L}^2 metric in the space of SRVFs is equivalent to the first two terms of Equation (6) when setting $a = 1$ and $b = \frac{1}{4}$. In our case, we define the Extended SRVF (ESRVF) of an edge x as the pair (q, r) where q is given by Equation (7), and $r(s)$ is the thickness of the edge at each point s . We can easily show that the \mathbb{L}^2 metric in the space of ESRVFs, denoted by Ω , is equivalent to the elastic metric of Equation (6) when setting $a = c = 1, b = \frac{1}{4}$. This is very important since, instead of working with the complex elastic metric, we can represent the shape of each edge in G using their ESRVFs and use the Quotient Euclidean Distance (QED) in the new tree-shape space, hereinafter referred to as the *ESRVF tree-shape space*, for comparing trees and computing geodesics. This new representation has the following properties;

- Since the ESRVF tree-shape space Ω is Euclidean, then the geodesics under the QED in the ESRVF tree-shape space are locally unique.
- The mapping between the tree-shape space to the ESRVF tree-shape space is surjective.
- The ESRVF map, i.e. the function Q which maps elements of X to Ω , is not injective, but two curves are mapped to the same ESRVF if and only if they are translates of each other.
- The inverse mapping has an analytical solution, see [SKJJ11]. In other words, for a given pair (q, r) , one can find, analytically and up to a translation, an edge x whose ESRVF is (q, r) .

In the following, we will first show how to compute geodesics under this new metric. Then, we demonstrate its application in the statistical analysis (Section 3) and 3D modeling, either automatically (Section 3.3) or interactively (Section 4), of 3D botanical trees.

Geodesics in the ESRVF tree-shape space. Since the full elastic metric is equivalent to the QED metric in the space of ESRVFs, computing geodesics under the ESRVF representation is straightforward and follows the same approach as in [WLY*18]; trees are first mapped to the ESRVF tree-shape space, geodesics are then computed under the QED metric, and the results are mapped back to the space of trees for visualization, see Figures 2-(a) and (b). Recall that both the mapping to the space of ESRVFs and the inverse

mapping have closed analytical forms. Also, although the ESRVF is not injective, i.e. two edges are mapped to the same ESRVF if and only if they are translates of each other (in other words, when mapping a pair (q, r) back to the tree-shape space, we lose the location of the edges), it is not an issue under the proposed tree parameterization. In our implementation, we first assume that the root edge is located at the origin. Mapping a pair (q, r) back to the tree-shape space will result in an edge e which is located at the origin. We thus translate it to the second end of its parent edge (i.e. the edge to which it is connected).

Figure 3 shows a simple example of two geodesics, one computed with the approach of Wang et al. [WLX*18] (left panel), and the other one using the elastic metric proposed in this article (right panel). In both cases, the intermediate trees along the geodesic are rendered in a semi transparent color. As one can see, in the approach of Wang et al. [WLX*18], the tree branches significantly shrink along the geodesic, while the approach we propose in this article clearly preserves the lengths of these branches.

Translation and scale invariance. The original SRVF framework of Srivastava et al. [SKJJ11] is invariant to translation. For scale invariance, the curves are scaled in such a way that they all have a unit length. However, scale invariance at the branch level is not desirable when comparing trees. In our case, we first translate all the trees so that the start point of their trunk is located at the origin. We then scale all the trees so that they fit within a sphere of radius one. At the branch level, we deactivate the scale normalization so that small branches can be deformed to big ones.

Correspondences. Central to computing geodesics is a mechanism for computing correspondences. For this purpose, we use the hierarchical procedure of [WLX*18]. The procedure assumes that trees are composed of a single trunk and many lateral branches. Each lateral branch contains many other sub-branches, and so on. If a tree is composed of multiple trunks then one is selected to be the main trunk and the others are treated as lateral branches. The upright orientation of the trees and their trunks are manually specified. In fact, this is the only manual interaction which is required. All the subsequent steps are automatic.

3. Statistical analysis

At this stage, we have all the necessary computational ingredients, which are a tree-shape space, an appropriate elastic metric, and a mechanism for computing correspondences and geodesics. In this section, we will show how to use these ingredients for the statistical analysis of the shape and the topological structure of 3D botanical trees, i.e. given a population of 3D botanical trees, we want to be able to compute the mean botanical tree and the modes of variations, characterize the population with probability distributions, and synthesize new botanical trees by sampling from these distributions. In the case of manifold 3D shapes that only bend and stretch, computing such quantities is straightforward by using standard tools from vector calculus [BV99], or advanced tools from differential geometry [LXS17]. Here, we focus on 3D botanical trees, which bend, stretch, and change their topological structure.

3.1. Averaging in the tree-shape space

Given a set of 3D botanical trees $\{\mathbf{x}_i \in X\}_{i=1}^n$, their mean tree is the point μ_x in the tree-shape space which is as close as possible, in terms of the metric, to all the points in the input set. It is defined as:

$$\mu_x = \arg \min_{\mathbf{x}} \sum_{i=1}^n [d_{geo}(\mathbf{x}, \mathbf{x}_i)]^2, \quad (8)$$

where $d_{geo}(\mathbf{x}, \mathbf{x}_i)$ is the length of the geodesic path which connects \mathbf{x} to \mathbf{x}_i . It is defined as

$$d_{geo}(\mathbf{x}, \mathbf{x}_i) = \inf_{\alpha} L[\alpha_{\mathbf{x} \rightarrow \mathbf{x}_i}], \quad (9)$$

where $L[\cdot]$ is given by Equation (3). As discussed in the previous section, working directly with the full elastic metric of Equation (6) is computationally very expensive. Instead, we propose to first map the trees into their ESRVF representation, compute the mean ESRVF using the QED metric, which is computationally more efficient, and then map the result back to the space of trees. Let \mathbf{q}_i be the ESRVF representation of a tree \mathbf{x}_i . The process of computing the mean tree starts by first finding the mean μ_q such that

$$\mu_q = \arg \min_{\mathbf{q}} \sum_{i=1}^n [d(\mathbf{q}, \mathbf{q}_i)]^2, \quad (10)$$

where $d(\mathbf{q}, \mathbf{q}_i)$ is the length of the geodesic between \mathbf{q} and \mathbf{q}_i , and it is computed using the QED metric. μ_q is then mapped back to the tree-shape space to find the mean tree μ_x . Feragen et al. [FLdB*13] showed that, under the QED metric, the function $E(q) = \sum_{i=1}^n [d(\mathbf{q}, \mathbf{q}_i)]^2$ is strictly convex. Thus, the mean, which is the minimizer of Equation (10), exists and is unique.

To solve this optimization problem, we use the weighted mid-points algorithm, which starts with a pair of trees, finds their average, and then iteratively updates the mean every time a new sample is added. This algorithm is general and does not depend on the order in which the input trees are processed. The general approach is summarized in Algorithm 1, which finds at the same time the correspondences between the trees and their statistical average with respect to the elastic metric.

3.2. Geodesic PCA

In addition to computing the mean tree of a collection of 3D botanical trees, we are interested in understanding (and modeling) how the geometry and the topological structure of botanical trees vary within the collection. The standard procedure can be summarized as follows;

- Compute the mean tree μ and register all the trees \mathbf{x}_i in the collection to the mean tree.
- Project all the points \mathbf{x}_i onto the tangent space to X at the mean (via the inverse exponential map). Let $T_\mu(X)$ denote this tangent space, which is Euclidean.
- Compute the covariance matrix of the population in $T_X(\mu)$, and its eigen decomposition (eigenvalues and eigenvectors).
- Each eigenvector in $T_X(\mu)$ can be converted into a geodesic principal curve by shooting a geodesic in the direction of the eigenvector.

Algorithm 1: Joint registration and averaging.*Input:* The set of trees $\{\mathbf{x}_1, \dots, \mathbf{x}_n\} \in X$.*Output:* Mean tree μ .

- 1: For each $i = 1, \dots, n$, normalize \mathbf{x}_i for translation and scale, and compute its ESRVF representation \mathbf{q}_i .
- 2: Set $U = \{\mathbf{q}_1, \dots, \mathbf{q}_n\}$, and set $j = 1$.
- 3: Select two points \mathbf{q}_i and \mathbf{q}_j , and set $V = U - \{\mathbf{q}_i, \mathbf{q}_j\}$.
- 4: Compute the geodesic between \mathbf{q}_i and \mathbf{q}_j , and set the mean μ_q to be the midpoint of the geodesic.
- 5: While $V \neq \emptyset$ do
 - Select a point \mathbf{q} from V . Let $V \leftarrow V - \{\mathbf{q}\}$.
 - Put μ_q and \mathbf{q} in correspondence, and compute the geodesic which connects them.
 - Let a be the length of this geodesic.
 - Set the new μ_q to be the point that is at $\frac{a}{j+2}$ from μ_q .
 - $j \leftarrow j + 1$.
- 6: Map μ_q back to the tree-shape space to obtain the mean tree μ .

Again, the main challenge with this standard approach is the computational complexity of the full elastic metric. Similar to the approach for computing the mean, since the QED metric in the ESRVF tree-shape space is equivalent to the elastic metric in the tree-shape space, we first map all the points to the ESRVF tree-shape space, perform geodesic Principal Component Analysis (PCA) in that space, and map the results back to the tree-shape space. Let μ_q be the mean in the ESRVF tree-shape space, computed using Algorithm 1. The covariance matrix C is given by:

$$C = \frac{1}{n-1} \sum_{i=1}^n \left(\text{Exp}_{\mu_q}^{-1}(\mathbf{q}_i) \right)^T \left(\text{Exp}_{\mu_q}^{-1}(\mathbf{q}_i) \right), \quad (11)$$

where $\text{Exp}_{\mu_q}^{-1}(\mathbf{q})$ is the inverse exponential map, which takes elements of Ω and maps them to the tangent space to Ω at μ_q . By computing the eigenvalues and eigenvectors of C , we can get the principal modes of variation of these input trees. Let $\lambda_k, \Lambda_k, k = 1, \dots, N$, be, respectively, the N leading eigenvalues (variances) and their associated principal directions. The principal directions Λ_k form an orthonormal basis. Any point \mathbf{q} in the ESRVF tree-shape space can be parameterized with a real-valued vector $(\alpha_1, \dots, \alpha_N)$ such that

$$\mathbf{q} = \text{Exp}_{\mu_q} \left(\sum_{i=1}^N \alpha_i \cdot \Lambda_i \right), \quad (12)$$

where Exp_{μ_q} is the exponential map, which takes elements of the tangent space to Ω at μ_q and maps them back to Ω . The final botanical tree can be obtained by mapping \mathbf{q} back to the tree-shape space.

3.3. Random generation of 3D tree models

Next, one can characterize the population $U = \{\mathbf{q}_1, \dots, \mathbf{q}_n\}$ by fitting probability distributions to the population. In general, any type of probability distributions can be fitted to the population since the ESRVF tree-shape space is equipped with the QED metric. In this article, for simplicity, we fit to the population a multivariate Gaus-

sian with mean μ_q and a diagonal covariance matrix Σ whose diagonal elements are the square roots of the eigenvalues λ_k .

Now, given the probability distribution model which characterizes the variability in the ESRVF tree-shape space, a new 3D botanical tree can be generated by sampling from the distribution. In the case of a Gaussian model, a random tree model \mathbf{x} can be obtained by first randomly generating N real values $\alpha_1, \dots, \alpha_N \in \mathbb{R}$ and setting

$$\mathbf{q} = \text{Exp}_{\mu_q} \left(\sum_{i=1}^N \alpha_i \sqrt{\lambda_i} \Lambda_i \right). \quad (13)$$

Finally, a botanical tree \mathbf{x} can be obtained by mapping \mathbf{q} back to the tree-shape space. In this article, we only consider the N -leading eigentrees chosen such that $\frac{\sum_{i=1}^N \lambda_i}{\sum_{i=1}^d \lambda_i} > 99\%$. (d is the total number of eigenvectors). Note that the larger $|\alpha_i \sqrt{\lambda_i}|$ is, the lower is the probability of the generated sample. Thus, in order to generate plausible trees, one can restrict α_i 's to be within a certain range, e.g. $[-1, 1]$.

4. Interactive 3D tree synthesis

In general, users would like to generate 3D trees by just specifying a few, say m , parameters. These parameters can be biologically motivated or extracted from 2D sketches drawn by the user on a sketching interface. In this article, we pursue the latter option and formulate the problem as a regression problem. In particular, let

- $\mathbf{p} \in \mathbb{R}^m$ be the vector of m parameters,
- \mathbf{x} be a point in the tree shape space and \mathbf{q} its corresponding representation in the ESRVF tree shape space. \mathbf{q} can be written in the form of Equation (12), and thus, it can be represented as a real valued vector $\mathbf{b} = (b_1, \dots, b_N)^T$.

We can assume that the relation between the parameters \mathbf{p} and the vector \mathbf{b} is linear, i.e.

$$\exists A, \text{ such that } A \times \mathbf{p} = \mathbf{b}. \quad (14)$$

Our goal is to learn the coefficients of the $N \times m$ matrix A from training samples. Let $\{\mathbf{x}_1, \dots, \mathbf{x}_n\}$ be our training samples, and $\{\mathbf{q}_1, \dots, \mathbf{q}_n\}$ their corresponding representations in the ESRVF tree-shape space. Let $\mathbf{b}^i = (b_1^i, \dots, b_N^i)^T$ be the vector representation of the i -th training sample \mathbf{q}_i , and \mathbf{p}^i its corresponding vector of parameters. Then, one can write:

$$A \times [\dots, \mathbf{p}^i, \dots] = [\dots, \mathbf{b}^i, \dots], \quad (15)$$

which can be written in the matrix form as:

$$A \times P = B. \quad (16)$$

Here, the unknown is the $N \times m$ matrix A . The matrix P is of size $m \times n$, and B is of size $N \times n$. If we are given a sufficient number of training samples, i.e. n is larger than $N \times m$, then the overdefined linear system of Equation (16) can be efficiently solved using the linear least squares method. At runtime, the user specifies a set of parameters \mathbf{p} , which are then used in Equation (14) to compute \mathbf{b} , which in turn is used in Equation (12) to generate a point \mathbf{q} in the ESRVF tree-shape space. Finally, a new botanical tree \mathbf{x} is generated by mapping \mathbf{q} back to the tree-shape space.

There are several ways of specifying the parameters \mathbf{p} . For instance, one can use biological parameters if appropriate training data is available. In our case, we have explored two sketch-based approaches. In the first approach, the user sketches a 2D contour representing the tree's crown. We discretize the 2D contour, save the coordinates into the parameter vector \mathbf{p} , and use it as input to Equation (14). In the second approach, the user only specifies the width and height of the convex hull of the tree's crown. In both approaches, we perform the training by taking 2D projections of the trees, and extract the 2D contour which bounds the tree's crown. We then apply a spline interpolation, and finally uniformly sample the spline curve to get points, which will be used as a vector of parameters \mathbf{p} for each training sketch. In the case of the second approach, we additionally extract the width and height of the convex hull of the 2D contours and use them to learn the regression model.

5. Results and applications

We demonstrate the performance of our framework using a dataset of eight species of 3D botanical trees with 10 to 70 tree models per species. Some of these trees have been created using modeling software such as Xfrog. Others have been downloaded from the internet. All the 3D models come with a known upright orientation. We will first compare the quality of the geodesics computed with the proposed approach and those computed using the approach of Wang et al. [WLX*18] (Section 5.1). Then, we show examples of summary statistics and examples of random trees automatically synthesized with the proposed framework (Section 5.2). Section 5.3 shows the use of regression in the ESRVF tree-shape space for the interactive synthesis of 3D trees using a 2D sketching interface. Finally, we report in Section 5.4 the computation time. Additional results are included in the supplementary material.

5.1. Geodesics

Figures 4 and 5 show a few examples of geodesics between the most left and the most right trees of each row. For each example, we show the geodesic computed using the approach of [WLX*18], which uses the QED metric in the tree-shape space, and the approach proposed in this article, which uses the elastic metric. In the examples of Figure 4 and Figure 5-(a) to (d), the branches of the source and target trees undergo large elastic deformations. Under such extreme deformations, the geodesics produced by [WLX*18] are not plausible since the intermediate trees along the geodesic shrink and then expand to match the target tree. This is not the case with the approach proposed in this article. Note also that, when the deformations between the source and target trees are small, as is the case with the examples of Figures 5-(e) and (f), both methods produce similar results.

User study. We conducted a user study on 50 participants, aiming to compare, in a quantitative manner, our method with the approach of Wang et al. [WLX*18]. Each participant is shown the geodesics of Figures 4 and 5, one at a time without knowing which one is generated with the approach of Wang et al. and which one is generated with our approach. The participants are then asked to assign to each geodesic a score between 0 and 10. The higher the score is, the better is the result from the participant view. We collected the

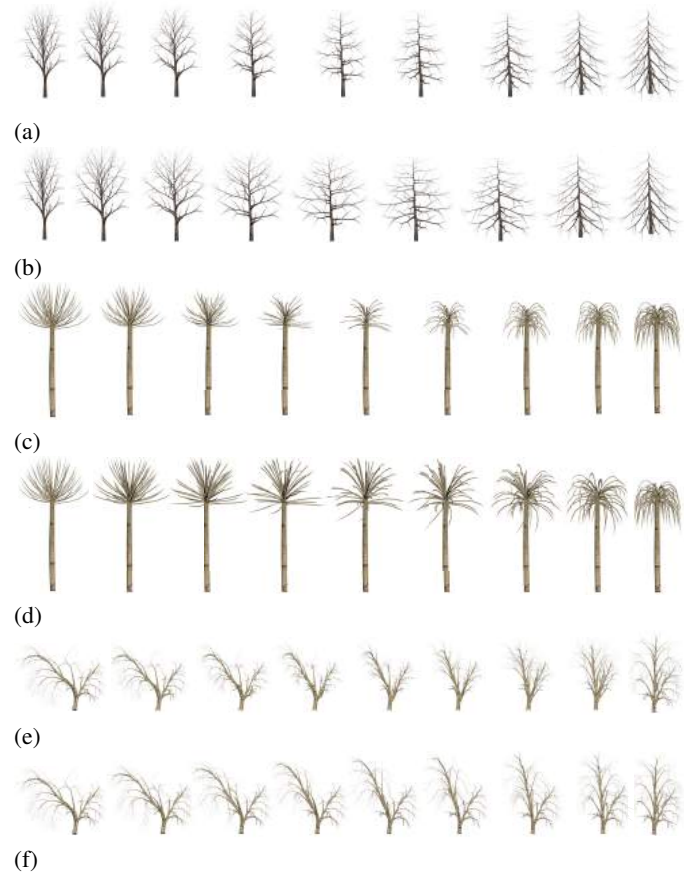


Figure 4: Comparison between geodesics computed using [WLX*18] (rows (a), (c), and (e)), which uses the QED metric in the tree-shape space, and using our approach (rows (b), (d), and (f)), which uses the elastic metric. Each row shows the geodesic between the most left and the most right trees.

scores and summarized them in Table 1. As one can see, all statistics show that the results produced with our method outperformed those of Wang et al. [WLX*18]. The supplementary material includes additional discussion about the results of the user study.

5.2. Statistical summaries and random trees generation

Figures 6 and 7 show examples of statistical analysis of the geometry and the topological structure of botanical trees. In each example, the panel (a) shows the 3D tree models used for training, while the panel (b) shows the mean tree (the 3D tree in the middle), which summarizes the input tree shapes, and the first three leading modes of variation. From these results, we clearly see that the first modes capture the main geometric and structural variations in the input tree models. The panel (c) of Figures 6 and 7 shows 3D tree models, which have been automatically synthesized by random sampling from the statistical model fitted to the trees shown in panel (a). These 3D trees, which have been synthesized without any biological knowledge or interaction from the user, share some similarities with the input trees but are not the same.

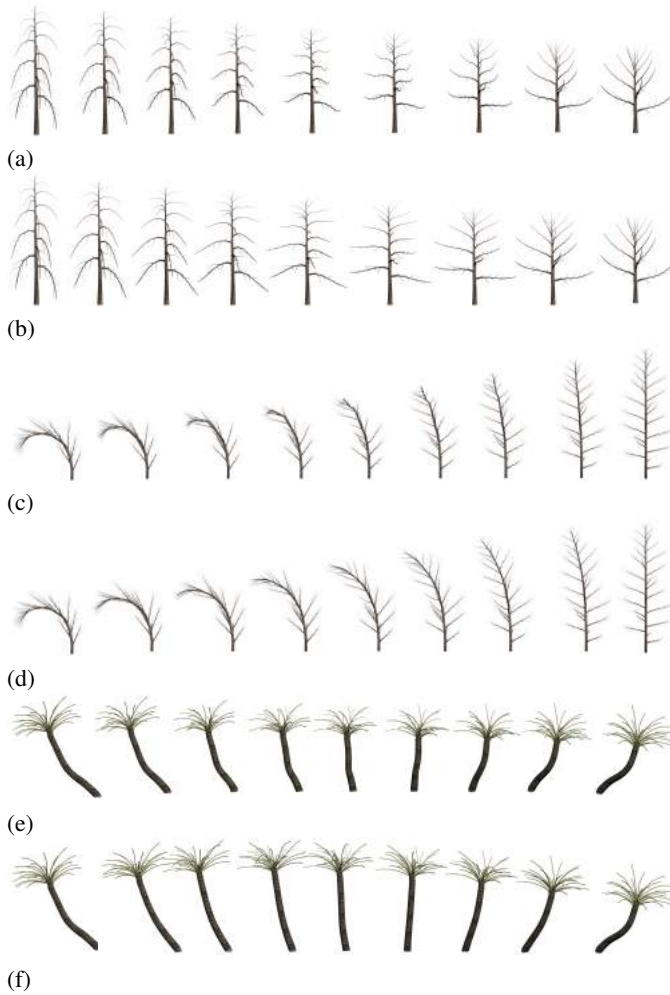


Figure 5: Comparison between geodesics computed using [WLX*18] (rows (a), (c), and (e)), which uses the QED metric in the tree-shape space, and using our approach (rows (b), (d), and (f)), which uses the elastic metric. Each row shows the geodesic between the most left and the most right trees.

In the examples of Figures 6 and 7, the input trees are all from the same species. Figure 8 shows the mean tree and the three leading modes of variation computed when mixing two species, namely the input trees of Figure 6 and Figure 1 of the supplementary material. Observe how the mean and the modes of variation summarize the main geometric and structural properties of both species. Figure 1-(a) shows examples of randomly synthesized trees by sampling from the probability distribution fitted to this mixed dataset. Figures 9 and 10 show other examples of statistic (mean, modes, and random trees) obtained by mixing two different species of trees.

5.3. Sketch-based 3D tree synthesis

We show a few examples of 3D trees created using the 2D sketching interface proposed in this article. We take the 3D tree models of each of the eight species used in this article, compute their

Table 1: Results of the user study. For each pair of geodesics (one generated with the approach of Wang et al. and another with the proposed approach), we report the average and median scores given by the participants. We also report in the last column the number of participants who voted for that geodesic as the best.

		Avg score	Median score	Best path votes
Figure 4	(a)-Wang et al.	6.88	7	12
	(b)-Our method	7.72	8	29
	(c)-Wang et al.	6.32	6	9
	(d)-Our method	7.52	8	29
	(e)-Wang et al.	6.98	7	12
	(f)-Our method	7.62	8	24
Figure 5	(a)-Wang et al.	7.08	7	13
	(b)-Our method	7.38	7	19
	(c)-Wang et al.	7.02	7	11
	(d)-Our method	7.66	8	23
	(e)-Wang et al.	6.94	7	16
	(f)-Our method	7.06	8	21

Table 2: Comparison of the timing (in seconds) for computing geodesics using our approach and the one of [WLX*18].

	Num. nodes	Num. edges	Wang et al. [WLX*18]	This article
Figure 4-(a), (b)	370	369	247.9	722.1
Figure 4-(c), (d)	106	105	20.8	87.6
Figure 4-(e), (f)	782	781	789.0	1214.7
Figure 5-(a), (b)	256	255	123.8	442.9
Figure 5-(c), (d)	836	835	1595.3	1862.6
Figure 5-(e), (f)	72	71	11.6	44.5

mean trees and their modes of variations, and then learn a regression model which maps 2D sketches into points in the tree-shape space. We consider the two input approaches described in Section 4; in the first approach, the user draws a 2D sketch and the system automatically synthesizes a 3D tree model. In the second approach, the user only specifies the width and height of the tree and the system synthesizes a new 3D tree model from these two parameters. Figure 1-(b) shows a at the same the 2D sketch drawn by the user and the 3D botanical tree synthesized by the proposed approach. Figure 11 shows a few more representative results produced with the two approaches. We also refer the reader to the supplementary material for additional results.

5.4. Computation time

The framework has been implemented in Matlab and runs on a desktop PC with Intel(R) Core(TM) i5 - 4570S CPU@2.90GHz and 8GB of RAM. Table 2 reports the computation time for each

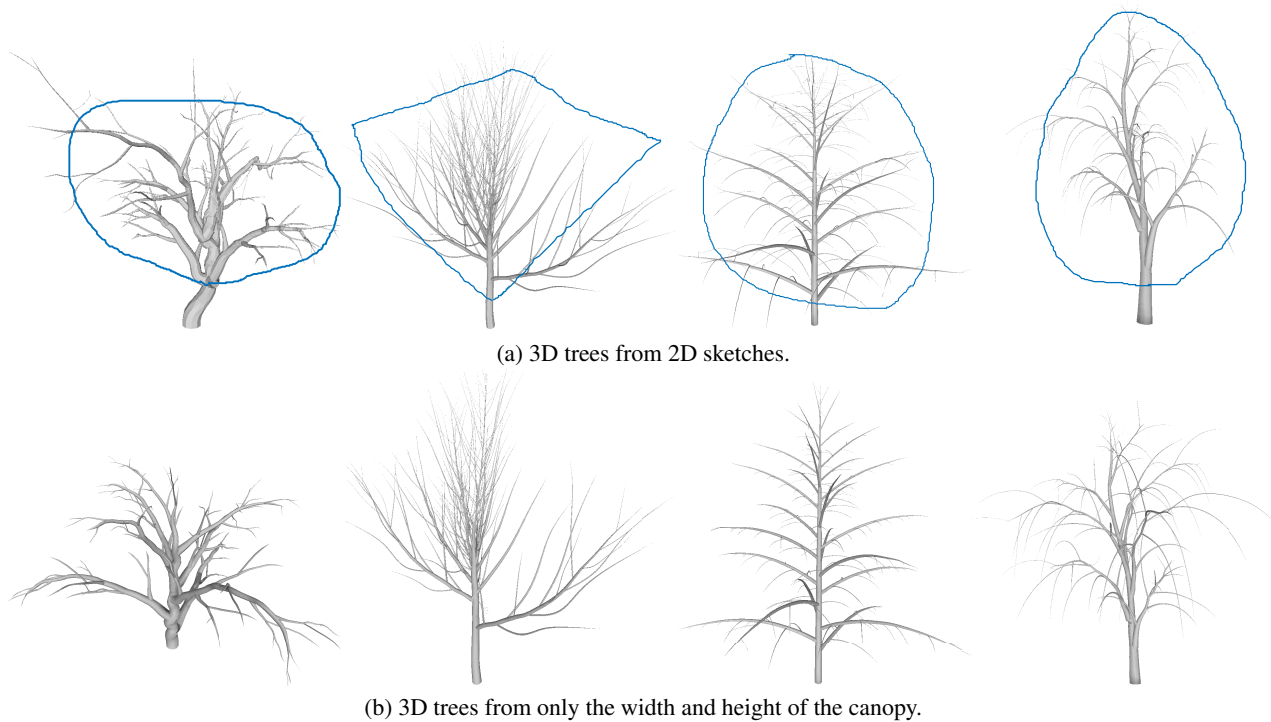


Figure 11: Examples of interactive 3D tree modeling using a 2D sketching interface. The user draws a 2D sketch, here shown in blue, and the system synthesizes the 3D geometry and topological structure of a botanical tree using as input (a) the 2D sketch, and (b) only the width and height of the bounding box of the 2D sketch.

Table 3: Breakdown of the computation time (in seconds) for the statistical analysis proposed in this article. Random sampling refers to the time needed to synthesize one botanical tree.

	Num. Train. samples	Mean	Modes	Random Sampling
Figures 1 and 8	12	24.75	899.5	26.7
Figure 6	21	10.8	359.8	12.4
Figure 7	78	29.2	1064.5	31.5

of the geodesics shown in this article. It also reports the size of the trees (in terms of the number of nodes and edges) and compares the timing with the approach of Wang et al. [WLX*18]. In summary, the approach of Wang et al. [WLX*18] is slightly faster than the one proposed in this article since the QED metric is essentially an Euclidean metric. Our approach is only slightly slower, since the elastic metric reduces to a QED metric in the ESRVF tree-shape space. The computation overhead is due to the mapping of the trees into the of ESRVF tree-shape space and the mapping of the results back to the space of trees for visualization.

Table 3 reports the computation time for each of the statistical analysis examples reported in this article. As one can see, the slowest example is the one of Figure 7, which required 50 seconds to compute the mean tree, 26 minutes to compute the modes of variation, and 52 seconds to synthesize one random botanical tree. Note

that the first two steps, i.e. the computation of the mean tree and the modes of variation, are offline steps. They are executed only once for the collection of botanical tree samples.

Finally, the regression step is instantaneous and requires less than 13 seconds for generating one 3D tree model from a 2D sketch.

6. Summary and future work

We have proposed a framework for generating new 3D tree models via statistical analysis of populations of botanical trees in the tree-shape space. It builds on and extends the framework of Wang et al. [WLX*18] in three aspects. First, we replace the QED metric by the full elastic metric, which yield into more plausible geodesics especially between pairs of trees which undergo large elastic and structural deformations. Second, we introduced methods for computing summary statistics (means and modes of variations) and for exploring the tree-shape space. Finally, we applied the framework to 3D botanical tree synthesis either randomly or interactively via a 2D sketching interface. The approach is fast and does not require biological expertise from the user. Moreover, it greatly simplifies the process of creating complex 3D botanical trees. To the best of our knowledge, this is the first approach that dealt with the statistical modeling of the 3D geometry and topological structure of trees.

Though effective as evidenced by the results and the experimental evaluations, there are several avenues for future work. First, the

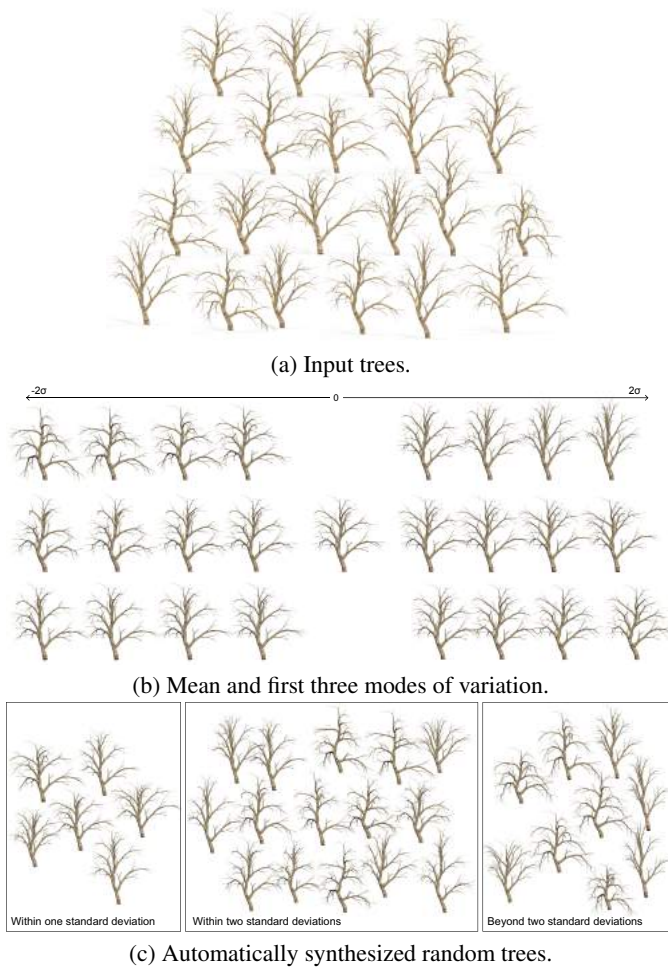


Figure 6: Statistical analysis of the input botanical trees in (a). In (b), we show the first three leading modes of variation. The highlighted tree in (b) corresponds to the mean of the trees in (a).

ability to compute geodesics in the ESRVF tree-shape space is very important. In fact, geodesics are the building block for statistical analysis. However, growth, disease progression, and deformation patterns in general, do not correspond to geodesics (which are the equivalent to straight lines in Euclidean spaces) but to curves in general. We plan to explore in the future how to fit curves and perform non-linear interpolations in the ESRVF tree-shape space.

Second, we used the Gaussian model to characterize variations in a collections of botanical trees. In general, these variations can be nonlinear and multimodal. In that case, it will be interesting to explore how to fit general distribution functions (e.g. Gaussian Mixture Models) to populations of trees in the ESRVF tree-shape space. Third, the sketching interface proposed in this article, although powerful and convenient, is just a proof of concept of regression in the ESRVF tree-shape space. In this article, we synthesize trees from a few geometric parameters (e.g. the convex hull of the tree). The approach, however, is general. For instance, one can

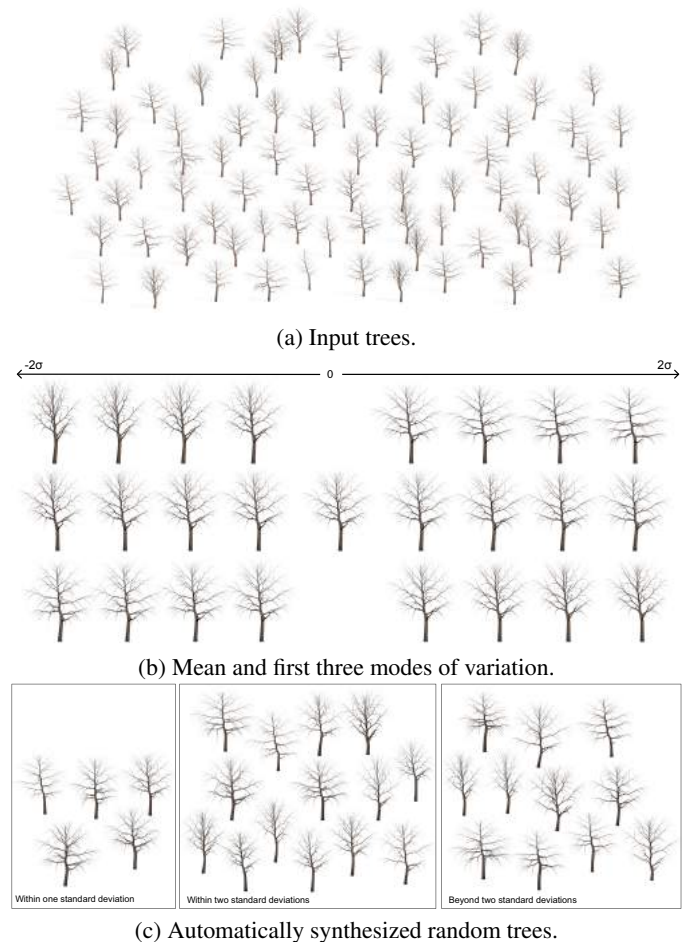


Figure 7: Statistical analysis of the input botanical trees in (a). In (b), we show the first three leading modes of variation. The highlighted tree in (b) corresponds to the mean of the trees in (a).

use the same approach to learn regression models to synthesize 3D trees from biological parameters if such training data is available.

Fourth, the proposed approach is data-driven; It does not incorporate any biological knowledge or parameters into the modeling process. This contrasts with most of the previous work, which attempt to explicitly model the biological processes underlying the development of botanical trees. The advantage of data-driven approaches is that they do not require any expertise from the user. Instead, they implicitly infer biological rules from data. The downside, however, is that they can only learn what is in the training data and thus they often require large training datasets with large variability. Also, the approach does not take into account competition for resources as well as external factors such effects of light, wind, or obstacles. It will be interesting to explore in the future whether hybrid approaches would benefit from the potential of data-driven as well as biologically-motivated families of techniques.

Finally, the proposed framework only considers the tree branches and ignores the leaves. Leaves can be easily synthesized on the gen-

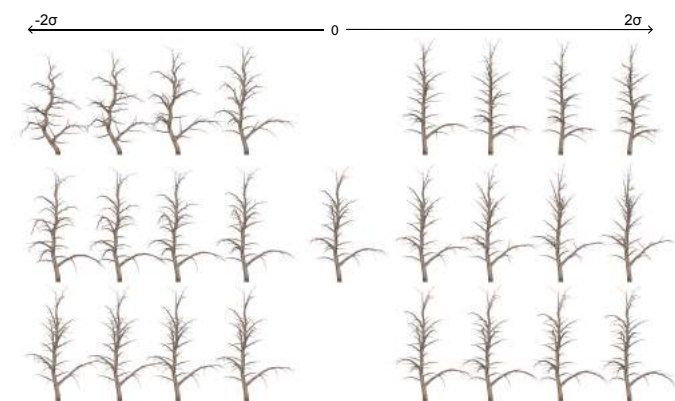
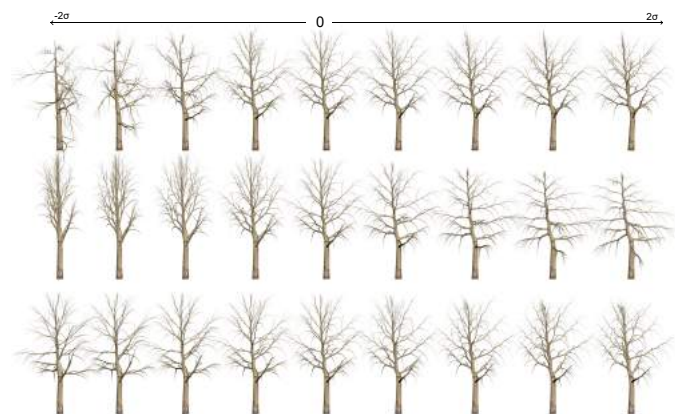
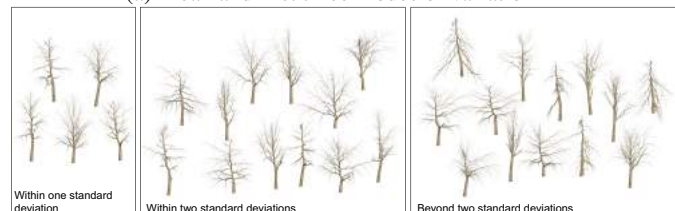


Figure 8: Statistical analysis (mean and first three modes of variation) of botanical trees belonging to two different species.



(a) Mean and first three modes of variation

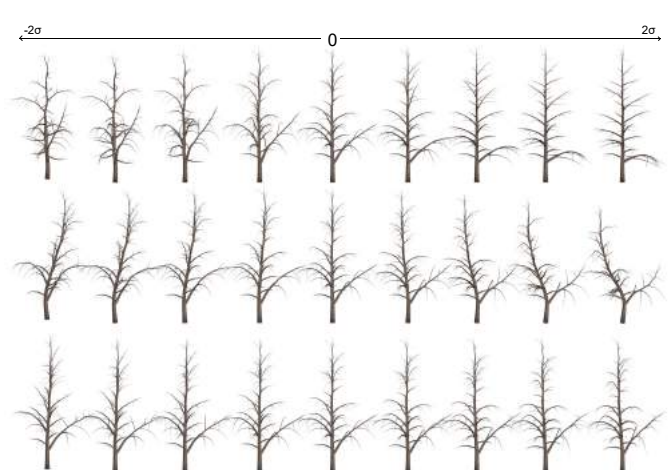


(b) Automatically synthesized random trees.

Figure 9: Statistical analysis (mean and modes of variation) of botanical trees from two different species (input trees of Fig. 7 mixed with the input trees of Fig. 2 of the supplementary material).

erated trees as commonly done in most of the previous works, e.g. [BNB13, WLX*18]. It will be interesting to extend the proposed statistical model to capture the foliage geometry and structure.

Acknowledgement. The authors would like to thank Anuj Srivastava for sharing the code for analyzing curves using Square Root Velocity Functions, and Aasa Feragen for making the code for tree-like shape analysis publicly available. Guan Wang would like to thank the China Scholarship Council for funding his vis-



(a) Mean and first three modes of variation



(b) Automatically synthesized random trees.

Figure 10: Statistical analysis (mean and modes of variation) of botanical trees belonging to two different species (input trees of Figure 1 and Figure 2 of the supplementary material).

it and stay at Murdoch University. This work was supported in part by the National Natural Science Foundation of China under Project 61602088, the Fundamental Research Funds for the Central Universities under Project A03017023701285, 2100219066, and 0200219153.

References

- [AAV*14] ALFARO C. A., AYDIN B., VALENCIA C. E., BULLITT E., LADHA A.: Dimension reduction in principal component analysis for trees. *Computational Statistics & Data Analysis* 74 (2014), 157–179. [3](#)
- [ACP03] ALLEN B., CURLESS B., POPOVIĆ Z.: The space of human body shapes: reconstruction and parameterization from range scans. In *ACM transactions on graphics* (2003), vol. 22, ACM, pp. 587–594. [2, 3](#)
- [AXZ*15] ALHASHIM I., XU K., ZHUANG Y., CAO J., SIMARI P., ZHANG H.: Deformation-driven topology-varying 3d shape correspondence. *ACM Transactions on Graphics (TOG)* 34, 6 (2015), 236. [3](#)
- [BHV01] BILLERA L. J., HOLMES S. P., VOGTMANN K.: Geometry of the space of phylogenetic trees. *Advances in Applied Mathematics* 27, 4 (2001), 733–767. [3](#)
- [BL08] BUCKSCH A., LINDENBERGH R.: Campinoła skeletonization method for point cloud processing. *ISPRS journal of photogrammetry and remote sensing* 63, 1 (2008), 115–127. [2](#)
- [BNB13] BRADLEY D., NOWROUZEZAHRAI D., BEARDSLEY P.: Image-based reconstruction and synthesis of dense foliage. *ACM Transactions on Graphics (TOG)* 32, 4 (2013), 74. [12](#)
- [BV99] BLANZ V., VETTER T.: A morphable model for the synthesis of 3d faces. In *Siggraph* (1999), pp. 187–194. [2, 3, 6](#)

- [CLM*11] COURNEDE P.-H., LETORT V., MATHIEU A., KANG M. Z., LEMAIRE S., TREVEZAS S., HOULLIER F., DE REFFYE P.: Some parameter estimation issues in functional-structural plant modelling. *Mathematical Modelling of Natural Phenomena* 6, 2 (2011), 133–159. 2
- [CNX*08] CHEN X., NEUBERT B., XU Y.-Q., DEUSSEN O., KANG S. B.: Sketch-based tree modeling using markov random field. *ACM Trans. Graph.* 27, 5 (Dec. 2008), 109:1–109:9. 2
- [FHN11] FERAGEN A., HAUBERG S., NIELSEN M., LAUZE F.: Means in spaces of tree-like shapes. In *Computer Vision (ICCV), 2011 IEEE International Conference on* (2011), IEEE, pp. 736–746. 4
- [FLdB*13] FERAGEN A., LO P., DE BRUIJNE M., NIELSEN M., LAUZE F.: Toward a theory of statistical tree-shape analysis. *IEEE trans. on PAMI* 35, 8 (2013), 2008–2021. 2, 3, 4, 5, 6
- [FLL*11] FERAGEN A., LAUZE F., LO P., DE BRUIJNE M., NIELSEN M.: Geometries on spaces of treelike shapes. *Computer Vision-ACCV 2010* (2011), 160–173. 4
- [FOP*13] FERAGEN A., OWEN M., PETERSEN J., WILLE M. M. W., THOMSEN L. H., DIRKSEN A., DE BRUIJNE M.: Tree-space statistics and approximations for large-scale analysis of anatomical trees. In *Information Processing in Medical Imaging* (2013), pp. 74–85. 2, 3
- [HBDP17] HÄDRICH T., BENES B., DEUSSEN O., PIRK S.: Interactive modeling and authoring of climbing plants. In *Computer Graphics Forum* (2017), vol. 36, Wiley Online Library, pp. 49–61. 3
- [IMIM08] IJIRI T., MECH R., IGARASHI T., MILLER G.: An example-based procedural system for element arrangement. In *Computer Graphics Forum* (2008), vol. 27, Wiley Online Library, pp. 429–436. 2
- [JKLS17] JERMYN I. H., KURTEK S., LAGA H., SRIVASTAVA A.: Elastic shape analysis of three-dimensional objects. *Synthesis Lectures on Computer Vision* 12, 1 (2017), 1–185. 3
- [KSKL13] KURTEK S., SRIVASTAVA A., KLASSEN E., LAGA H.: Landmark-guided elastic shape analysis of spherically-parameterized surfaces. *Comp. Graph. Forum* 32, 2pt4 (2013), 429–438. 3
- [LD99] LINTERMANN B., DEUSSEN O.: Interactive modeling of plants. *IEEE Computer Graphics and Applications* 19, 1 (1999), 56–65. 2
- [LDS*11] LI C., DEUSSEN O., SONG Y.-Z., WILLIS P., HALL P.: *Modeling and generating moving trees from video*, vol. 30. ACM, 2011. 2
- [Lin68] LINDENMAYER A.: Mathematical models for cellular interactions in development i. filaments with one-sided inputs. *Journal of theoretical biology* 18, 3 (1968), 280–299. 2
- [LKSM14] LAGA H., KURTEK S., SRIVASTAVA A., MIKLAVCIC S. J.: Landmark-free statistical analysis of the shape of plant leaves. *Journal of theoretical biology* 363 (2014), 41–52. 2
- [LRBP12] LONGAY S., RUNIONS A., BOUDON F., PRUSINKIEWICZ P.: Treesketch: interactive procedural modeling of trees on a tablet. In *Proceedings of the international symposium on sketch-based interfaces and modeling* (2012), Eurographics Association, pp. 107–120. 2
- [LXJS17] LAGA H., XIE Q., JERMYN I. H., SRIVA A.: Numerical inversion of snrf maps for elastic shape analysis of genus-zero surfaces. *IEEE Trans. on Pattern Analysis and Machine Intelligence* 39, 12 (2017), 2451–2464. doi:10.1109/TPAMI.2016.2647596. 2, 3, 6
- [LYO*10] LIVNY Y., YAN F., OLSON M., CHEN B., ZHANG H., EL-SANA J.: Automatic reconstruction of tree skeletal structures from point clouds. *ACM Transactions on Graphics (TOG)* 29, 6 (2010), 151. 2
- [MVG13] MARTINOVIC A., VAN GOOL L.: Bayesian grammar learning for inverse procedural modeling. In *Proceedings of the IEEE Conference on Computer Vision and Pattern Recognition* (2013), pp. 201–208. 2
- [OOI07] OKABE M., OWADA S., IGARASHI T.: Interactive design of botanical trees using freehand sketches and example-based editing. In *ACM SIGGRAPH 2007 courses* (2007), ACM. 2
- [OP11] OWEN M., PROVAN J. S.: A fast algorithm for computing geodesic distances in tree space. *IEEE/ACM Transactions on Computational Biology and Bioinformatics* 8, 1 (2011), 2–13. 3
- [PBI*16] PIRK S., BENES B., IJIRI T., LI Y., DEUSSEN O., CHEN B., MĚCH R.: Modeling plant life in computer graphics. In *ACM SIGGRAPH 2016 Courses* (2016), ACM, p. 18. 2
- [PBPS99] POWER J. L., BRUSH A. J. B., PRUSINKIEWICZ P., SALESIN D. H.: Interactive arrangement of botanical l-system models. In *Proceedings of the 1999 symposium on Interactive 3D graphics* (1999), ACM, pp. 175–182. doi:10.1145/300523.300548. 2
- [PGW*04] PFEIFER N., GORTE B., WINTERHALDER D., ET AL.: Automatic reconstruction of single trees from terrestrial laser scanner data. In *ISPRS Congress* (2004), ISPRS Istanbul, pp. 114–119. 2
- [PHHM96] PRUSINKIEWICZ P., HAMMELY M., HANANZ J., MECH R.: L-system: From the theory to visual models of plants. *CSIRO Symposium on Computational Changes in Life Sciences* (1996). 2
- [PMKL01] PRUSINKIEWICZ P., MÜNDERMANN L., KARWOWSKI R., LANE B.: The use of positional information in the modeling of plants. In *Siggraph* (2001), ACM, pp. 289–300. 2
- [PNH*14] PIRK S., NIESE T., HÄDRICH T., BENES B., DEUSSEN O.: Windy trees: computing stress response for developmental tree models. *ACM Transactions on Graphics (TOG)* 33, 6 (2014), 204. 3
- [PSK*12] PIRK S., STAVA O., KRATT J., MASSIH SAID M. A., NEUBERT B., MECH R., BENES B., DEUSSEN O.: Plastic trees: interactive self-adapting botanical tree models. *ACM TOG* 31, 4 (2012), 1–10. 2
- [PSTV09] PRATIKAKIS I., SPAGNUOLO M., THEOHARIS T., VELTKAMP R.: Skeltre-fast skeletonisation for imperfect point cloud data of botanic trees. 2
- [Q TZ*06] QUAN L., TAN P., ZENG G., YUAN L., WANG J., KANG S. B.: Image-based plant modeling. In *ACM Transactions on Graphics (TOG)* (2006), vol. 25, ACM, pp. 599–604. 2
- [QYH*17] QUIGLEY E., YU Y., HUANG J., LIN W., FEDKIW R.: Real-time interactive tree animation. *IEEE transactions on visualization and computer graphics* (2017). 3
- [RLM07] RUDNICK S., LINSSEN L., MCPHERSON E. G.: Inverse modeling and animation of growing single-stemmed trees at interactive rates. 2
- [ŠBM*10] ŠTAVA O., BENEŠ B., MĚCH R., ALIAGA D. G., KRIŠTOF P.: Inverse procedural modeling by automatic generation of l-systems. In *Computer Graphics Forum* (2010), vol. 29, Wiley Online Library, pp. 665–674. 2, 3
- [SKJJ11] SRIVASTAVA A., KLASSEN E., JOSHI S. H., JERMYN I. H.: Shape analysis of elastic curves in euclidean spaces. *IEEE Trans. on Pattern Analysis & Machine Intelligence* 33, 7 (2011), 1415–1428. 5, 6
- [SPK*14] STAVA O., PIRK S., KRATT J., CHEN B., MĚCH R., DEUSSEN O., BENES B.: Inverse procedural modelling of trees. In *Computer Graphics Forum* (2014), vol. 33, Wiley Online Library, pp. 118–131. 2, 3
- [TFX*08] TAN P., FANG T., XIAO J., ZHAO P., QUAN L.: Single image tree modeling. *ACM Transactions on Graphics* 27, 5 (2008), 108. 2
- [TYK*12] TALTON J., YANG L., KUMAR R., LIM M., GOODMAN N., MĚCH R.: Learning design patterns with bayesian grammar induction. In *Proceedings of the 25th annual ACM symposium on User interface software and technology* (2012), ACM, pp. 63–74. 2
- [WBCG09] WITHER J., BOUDON F., CANI M.-P., GODIN C.: Structure from silhouettes: a new paradigm for fast sketch-based design of trees. In *Computer Graphics Forum* (2009), vol. 28, Wiley Online Library, pp. 541–550. 2
- [WLX*18] WANG G., LAGA H., XIE N., JIA J., TABIA H.: The shape space of 3d botanical tree models. *ACM Trans. Graph.* 37, 1 (Jan. 2018), 7:1–7:18. doi:10.1145/3144456. 2, 3, 4, 5, 6, 8, 9, 10, 12
- [WXJD17] WANG Y., XUE X., JIN X., DENG Z.: Creative virtual tree modeling through hierarchical topology-preserving blending. *IEEE transactions on visualization and computer graphics* 23, 12 (2017), 2521–2534. 3

- [ZHRS15] ZHANG C., HEEREN B., RUMPF M., SMITH W. A.: Shell p-ca: statistical shape modelling in shell space. In *ICCV* (2015), pp. 1671–1679. [3](#)
- [ZXLJ15] ZHANG D., XIE N., LIANG S., JIA J.: 3d tree skeletonization from multiple images based on pyrkl optical flow. *Pattern Recognition Letters* (2015). [4](#)